https://dx.doi.org/10.21577/0103-5053.20230009

J. Braz. Chem. Soc., Vol. 34, No. 7, 967-975, 2023

Article

Study of Manganese Laurate as Adsorbing Matrix for Undecan-2-one: Factors Affecting Adsorption for Application in Controlled-Release of Pheromones

Anderson N. de Carvalho,[a] Mirelly A. V. Fonseca,[a] Diogo M. Vidal,[b] Ana C. T. Cursino,[c] Daniele S. Firak[d] and Fábio S. Lisboa *,[a]

[a]*Instituto de Física e Química, Universidade Federal de Itajubá (UNIFEI), Campus Itajubá, 37500-903 Itajubá-MG, Brazil*

[b]*Departamento de Química, Instituto de Ciências Exatas, Universidade Federal de Minas Gerais (UFMG), 31270-901 Belo Horizonte-MG, Brazil*

[c]*Departamento de Química, Universidade Tecnologica Federal do Paraná (UTFPR), Campus Medianeira, 85884-000 Medianeira-PR, Brazil*

[d]*Atmospheric Chemistry Department, Leibniz Institute for Tropospheric Research (TROPOS), Permoserstraße 15, 04318 Leipzig, Germany*

One of the greatest challenges faced by agriculture is the use of agrochemicals and the balance between food production and environmental problems associated with the excessive use of these substances. To overcome this issue, pheromones have been used to trap pests that harm crops. This work reports the use of a layered monocarboxylate, manganese laurate (MnL_2), as adsorbing matrix for undecan-2-one (methyl nonyl ketone (MNK)), one of the components of the pheromone of the insect *Lobiopa insularis*, which is a pest in the strawberry cultivar. The manganese laurate was synthesized by a coprecipitation method and was later characterized using X-ray diffractometry, vibrational spectroscopy, thermogravimetric analysis, and differential scanning calorimetry. The characterization techniques showed that MNK was adsorbed in the manganese laurate structure in a range of 0.08 to 1.13 mg g^{-1}, and this interaction was investigated in a factorial design experiment, in which the variables temperature, time of contact, and matrix:MNK ratio were investigated. A negative effect of increasing temperatures was observed and attributed to substrate volatilization. The adsorption was favored in increasing molar ratios and times of contact, and ideal conditions for the adsorption could be found, indicating that manganese laurate could be applied in controlled-release tests.

Keywords: layered compounds, layered monocarboxylates, undecan-2-one, *Lobiopa insularis*, adsorbing materials

Introduction

Different species of arthropods have become agricultural pests in the last decades, causing great problems in many types of plantations around the world. This situation is more worrisome in countries with a huge part of their economy reliant on agriculture. In Brazil, for instance, many food crop cultivars have been damaged by pests and one of great concern is the strawberry cultivar.[1] According to IBGE (Brazilian Institute of Geography and Statistics), 2017,[2] the strawberry production in Brazil is concentrated in the region of Minas Gerais, which is responsible for about 66% of the total production.

The most important pest in strawberry cultivars is the beetle *Lobiopa insularis* (Coleoptera: Nutidulidae), which can lead to high losses of production that can reach values as great as 70%.[3] This directly affects the economy of the region, causing an increase in the market price and a decrease in the profits of the producers. To control the *L. insularis* insect and minimize production losses, agrochemicals are applied in plantations; however, the use of these types of chemicals has potential environmental toxicity and can damage human health.[4]

One way to avoid or decrease the use of agrochemicals is the introduction of technologies based on pheromones

*e-mail: fabiolisboa@unifei.edu.br
Editor handled this article: Ivo M. Raimundo Jr. (Associate)

to control pests. One interesting application is based on trapping insects using attracting pheromones as lures. Another possibility would be the interruption of the species courtship cycle by suturing the environment with a pheromone component. In the case of *Lobiopa insularis*, a mixture of undecan-2-one (methyl nonyl ketone (MNK)), nonan-2-one, and undecan-2-ol, in a proportion of 88:3:9, was found by Moliterno *et al*.[5] to be the composition of a male-produced aggregation pheromone released by this insect.

Some drawbacks in the use of pheromones are in the handling and storage of the materials, mostly because of the volatility of the compounds present in a pheromone or even because of their chemical instability in the presence of electromagnetic radiation.[6] A strategy to avoid or reduce these issues is the incorporation of pheromone molecules into a compatible matrix.[7]

A class of materials that can be applied as matrices for incorporating molecules (including pheromones) are the layered compounds, which can allocate different species in the interlayer space.[8] Different compounds, like layered double hydroxides (LDH), layered hydroxysalts (LHS), dichalcogenides, and kaolinite can act as matrices for host species, thus forming what is known as an intercalation compound.[9] Layered materials can incorporate a great variety of atoms, molecules, and ions in their interlayer space and can also release these species at slow rates; for example, Borges *et al*.[10-12] used clay minerals and two LDH (MgFe and MgAl) as matrices for the slow release of fertilizers.

Another class of layered compounds of great interest is the layered metal monocarboxylates, also called metallic soaps. They are derived from saturated or unsaturated fatty acids, and some applications include acting as lubricating materials, catalysts, pigments, and fungicides.[13-16] These type of materials have a general formula $M^{y+}(C_nH_{2n+1}COO)_y$, in which each layer are formed by bilayers of carboxylates groups coordinated to metal ions in bridging bidentate mode, while the saturated organic chains are in all-*trans* conformation.[17,18]

Saturated metal monocarboxylates in layered structures display an amazing behavior when heated at low temperatures: they form mesophases and micelles.[19,20] This performance can help the metal carboxylates to absorb non-polar or low-polarity organic molecules by exposing the saturated organic chain in micellar form or favoring the entrance of molecules in the interlayer space by reducing the packing density.[21] If the molecular structure of the host and matrix are compatible, the intermolecular forces will favor adsorption; thus, chemical compatibility increases the probability of interaction.[22]

Regarding all that was mentioned above, saturated metal monocarboxylates in a lamellar organization are a promising alternative to adsorb molecules existing in pheromones composition. A valuable application is the adsorption of MNK, which is a saturated ketone with eleven carbons and a carbonyl group at the second carbon atom present in the pheromone of *Lobiopa insularis*.[5]

In this work, we used a saturated metal monocarboxylate (manganese laurate) for adsorption of MNK. The choice for the manganese laurate was because this compound presented the best results for MNK adsorption if compared to tests performed with other laurates, of copper, nickel, iron, lanthanum, and zinc (data not shown). This study had the objective to evaluate factors that influence interactions between the metal monocarboxylate and a pheromone component, MNK. The variables temperature, molar ratio matrix:MNK, and exposure time were investigated for future applications in the production of controlled-release materials for pest control in strawberry plantations.

Experimental

Synthesis of the metal monocarboxylate manganese laurate (MnL_2)

The manganese laurate was synthesized by a coprecipitation method in two steps.[14] Firstly, the sodium monocarboxylates were generated *in situ* by reacting lauric acid (22.04 mmol, 98% Sigma- Aldrich, St. Louis, USA) in ethanol (30 mL, 99.8% Vetec, Duque de Caxias-RJ, Brazil) with sodium hydroxide (22.04 mmol, 98% Vetec, Duque de Caxias-RJ, Brazil), previously solubilized in ethanol (20 mL) at 50 °C. The generated sodium monocarboxylate was solubilized with the addition of distilled water (50 mL) at 50 °C.[23] The second step was the slow addition (30 drops *per* min) of manganese chloride (11.02 mmol, 98% Dinâmica, Indaiatuba-SP, Brazil) solubilized in distilled water (50 mL) to the sodium laurate solution. The obtained light pink solid was washed several times with acetone (98% Dinâmica, Indaiatuba-SP, Brazil) and subsequently with distilled water, and it was later dried in a lab oven at 60 °C for 48 h.

Adsorption of MNK on the manganese laurate (MnL_2) matrix

A complete 2^3 factorial design of experiments with four replicates in the central point was employed to investigate the adsorption of MNK (Sigma-Aldrich 99.9%, St. Louis, USA) in the matrix. Table 1 presents the factor level settings for the design of experiments.

After preliminary investigations conducted by our

Table 1. Variables and factor level settings

Condition	Low (−1)	Standard (0)	High (+1)
Temperature / °C	90	100	110
Contact time / days	2	8	15
Molar ratio (matrix[a]:MNK)	1:10	1:30	1:50

[a]Manganese laurate (MnL_2); MNK: methyl nonyl ketone (undecan-2-one).

research group (data not shown), the adsorption of MNK in the carboxylate structure was found to be not favored in temperatures between 70 and 120 °C. The tested times in these studies were 1, 15, and 30 days. The time of 30 days was further disregarded because it did not show the presence of MNK in the matrix. With the adsorption time of 1 day, MNK was observed in the carboxylate matrix, but it was verified that the adsorption was higher after 2 days, and so the contact time of 1 day was consequently discarded. Thus, temperatures and reaction times applied in the present work were determined from these preliminary investigations.

The adsorption of MNK was made with the addition of manganese laurate (150 mg) into a 10 mL autoclave reactor, with an internal polytetrafluoroethylene (PTFE) vessel and an external stainless-steel body, and the addition of the desired amount of MNK. Then, the autoclave was tightly closed and placed in a lab oven at temperatures and contact times described in the factorial design table. After that, the solid was washed with acetone three times, dried at a desiccator for 30 min, and safely stored in a flask at room temperature.

To quantify the adsorbed MNK, the manganese laurate (50 mg) was digested with hydrochloric acid (10 mL, 37% PA Dinâmica, Indaiatuba-SP, Brazil) under an ice bath, and 10 mL of *n*-heptane was later added to separate the host species. The organic phase was separated and then analyzed in an ultraviolet-visible spectrometer, in the region from 250 to 600 nm.

Equipment

The Fourier transform infrared (FTIR) spectra were recorded in a PerkinElmer (Waltham, Massachusetts, USA) Spectrum 100 instrument, equipped with a diamond crystal for total attenuated reflectance (ATR) module, in the wavelength range of 650-4000 cm^{-1}, resolution of 4 cm^{-1}, and 16 scans. The X-ray diffractograms were obtained in a Malvern Panalytical X'Pert PRO (Malvern, UK), equipped with copper target (k_α = 1.5404 Å), at the following conditions: current of 30 mA, voltage of 40 kV, step of 0.02º, time *per* step of 0.5 s, and scan range from 3 to 70º of 2θ degrees. Thermogravimetric analyses (TGA) were made in a Mettler Toledo (Greifensee, Switzerland) equipment, model TG 50, with oxygen flow of 50 mL min^{-1} in a range of 30 to 1000 °C and heating rate of 10 °C min^{-1}. The differential scanning calorimetry (DSC) measurements were conducted at a Shimadzu (Tokyo, Japan) equipment, model DSC 60, with nitrogen flow of 50 mL min^{-1} in a range of 25 to 150 °C. The UV-Vis analyses were made at an ultraviolet-visible spectrometer, model Varian (California, USA) Cary 50 Bio, from 250 to 800 nm in a quartz cuvette.

Results and Discussion

Characterization of manganese laurate (MnL_2)

The X-ray powder diffraction (XRD) analysis (Figure 1) showed a characteristic layered profile for the synthesized manganese carboxylate. The basal distance obtained was 34.18 Å, and this distance is in agreement with the presence of organic chain bilayers forming the layered structure.[17,24]

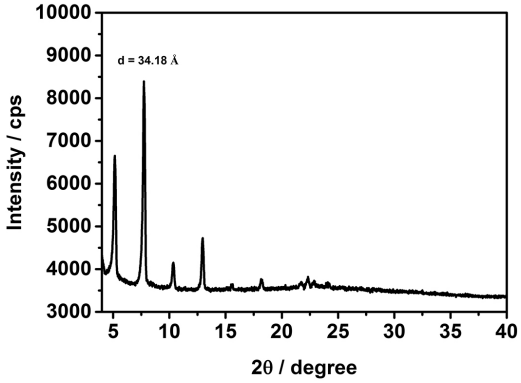

Figure 1. X-ray powder diffraction profile obtained for manganese laurate.

The vibrational spectroscopy in the near-infrared region (NIR) of the synthesized metal monocarboxylate, displayed in Figure 2a, exhibits expected vibrational modes compared with corresponding compounds reported in other works.[25]

The analysis of the spectra of manganese laurate (MnL_2) presented the following stretching modes: water molecules in the region of 3300-3000 cm^{-1}, CH_3 and CH_2 groups at 2955 and 2851 cm^{-1}, CH_2 rocking mode at 726 cm^{-1}, and asymmetrical and symmetrical COO^- stretching modes at 1559 and 1417 cm^{-1}. The latter results, referring to COO^- stretching modes, give a difference of wavenumber ($\Delta\nu$) of 142 cm^{-1}, coherent with a coordination mode like a bridging bidentate between the carboxylate groups and the two metallic centers.[26,27]

It is also possible to observe some bands in the region between 1100 and 1350 cm^{-1}; these bands are called progression bands and give the information that the organic chains are in all *trans* conformation.[17]

The Δν and progression bands help to understand the way the organic chains and metallic ions are organized in the layers and support the observed in the X-ray analysis. Table 2 summarizes the main vibrational modes obtained for the layered compound.

The thermogravimetric analysis is shown in Figure 2b. The decomposition profile for MnL_2 presented four mass loss events; the one next to 100 °C is relative to the presence of moisture as observed in the FTIR spectrum of this compound. A second and prominent event was observed at 300 °C, associated with the oxidation of the organic matter present in the composition of the MnL_2. The third (next to 380 °C) and fourth (900 °C) events determinate the total decomposition of the MnL_2 up to the oxide formation. As expected, the profile is characteristic of saturated metal monocarboxylates and the composition was estimated as $[Mn(CH_3(CH_2)_{10}COO)_2].H_2O$.[14]

The DSC graphic is shown in Figure 2c. This analysis presented curves for three distinct cycles of heating and cooling of the MnL_2. The curves showed four main events during the first heating cycle at temperatures of 85, 108, 113, and 143 °C. The intensity of the endothermic peak at 85 °C significantly decreases after the first cycle, and this event is probably caused by the loss of water in the hydrated phase and a mesophase formation.[28,29] The two next observed events, at 108 and 113 °C, are attributed to the other two new mesophases originated by the heating, while the exothermic peak at 143 °C represents the fusion process of the manganese laurate. In the first cooling cycle, three events are observed at 133, 90, and 65 °C; all these events are due to the recrystallization process of three different mesophases of the manganese laurate. In the second and third heating cycles, three events are observed at 78, 110, and 144 °C. The first event changes from 85 to 78 °C in the subsequent cycle, indicating that the hydrated phase is no longer present in the subsequent cycles. The event at 110 °C refers to the stabilization of one of those two mesophases observed at the first heat cycle, firstly observed at 108 and 113 °C, while the same three events observed in the first cooling cycle are repeated in the next cycles.

As previously described, those events refer to mesophase formation, fusion processes, and recrystallization. The variation observed in the peak positions (temperatures)

Table 2. Main vibrational modes observed for MnL_2

	Vibrational mode / cm^{-1}						
	OH	CH_3	CH_2	$\nu_a COO^-$	$\nu_s COO^-$	PB	$\Delta\nu_{(COO-)}$
MnL_2	3338	2917	2851 / 726	1559	1417	1331-1195	142

PB: progression bands.

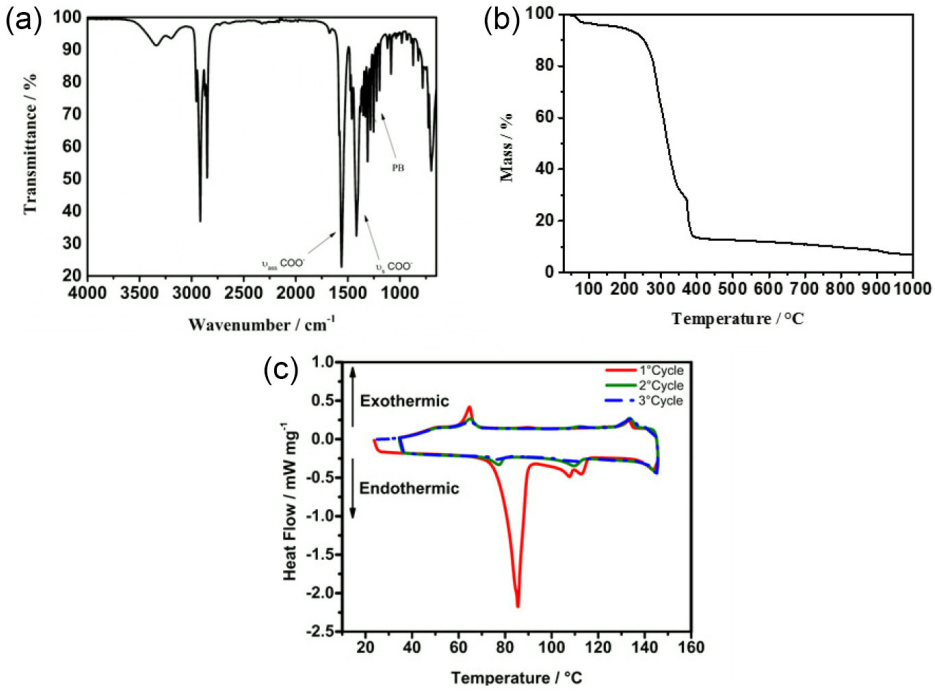

Figure 2. (a) FTIR (ATR) spectrum; (b) TGA and (c) DSC curves obtained for the MnL_2.

between the first and subsequent cycles were probably the result of a structural reorganization of the manganese laurate.[28,29] The mesophase formation is known to be related with the size and oxidation state of the metallic center coordinated to the monocarboxylate ion. Small ions form fewer stable structures because they keep the neighboring bidentate bridges formed by the carboxylates bound to the metallic center closer, which generates a repulsion among these groups that disfavors the formation of mesophases.[28]

The mesophases generated during the DSC process for this manganese monocarboxylate were not conclusively determined but are under investigation.

Adsorption tests of MNK on the manganese laurate (MnL_2) matrix

The MnL_2 presented the capacity to absorb MNK on its structure in all tested conditions. The XRD analysis (not shown) conducted with the solids after the adsorption tests showed no change in basal spacing, and this indicates that no intercalation or adsolubilization process occurred, therefore, the substrate was incorporated on the solid surface as will be discussed herein.

Figure 3 shows the FTIR profiles of the matrix before and after the interaction with the adsorbate molecules for tests at the condition of molar ratio (MnL_2:MNK) 1:50, 2 days, and temperatures of 90, 100, and 110 °C. All vibrational spectra resulting from adsorption tests showed the same profile exemplified in Figure 3.

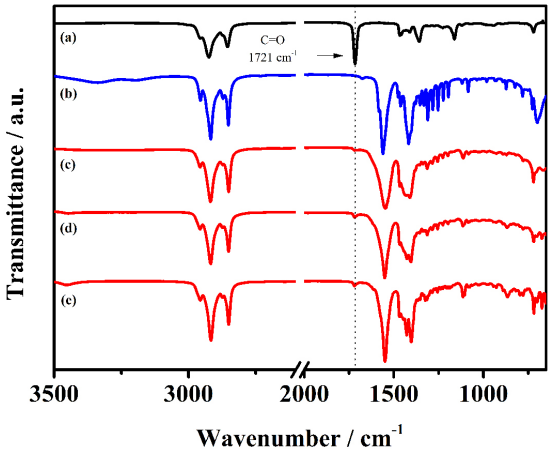

Figure 3. FTIR (ATR) analysis of the adsorption tests of MNK in the metal monocarboxylate matrix with molar ratio (MnL_2:MNK) 1:50, 2 days and described temperatures. (a) Undecan-2-one; (b) manganese laurate before adsorption reactions and MnL_2 after adsorption reactions at (c) 90, (d) 100 and (e) 110 °C.

Besides the presence of the metal-monocarboxylate vibrational bands previously discussed in this work (Figure 2a), in the spectra shown in Figure 3, it is possible to observe a new band at 1718 cm^{-1}, attributed to the carbonyl group (C=O) of the ketone group present in the MNK structure.[30,31]

After the extraction of the MNK from the monocarboxylate matrix, the UV-Vis spectra were collected (Supplementary Information section) and showed an absorption band at 275 nm, characteristic of the electronic transition $\pi \rightarrow \pi^*$ of carbonyl groups (C=O) for MNK, which also corroborates its presence on the matrix before extraction as observed in the FTIR spectra.[32]

Table 3 represents the experiments conducted in the factorial design, with answers given as the quantity of MNK obtained *per* gram of metal monocarboxylate matrix. The adsorption range varied from 0.0869 to 1.1310 mg g^{-1}. The last value was achieved at the lower temperature and the greater time of contact and molar ratio. A more detailed discussion will be made in the following paragraphs. According to the analysis of variance (ANOVA), the three main effects were significant, molar ratio, time of contact (written as factor "time"), and temperature. The Pareto chart of effects is provided in Figure 4.

Table 3. Factorial design experiments and responses are given as MNK adsorption in the manganese laurate

Contact time / days	Temperature / °C	Molar ratio (MnL_2:MNK)	Response / (mg g^{-1})
2	90	1:10	0.0869
15	90	1:10	0.1945
2	110	1:10	0.3027
15	110	1:10	0.2594
2	90	1:50	0.4512
15	90	1:50	1.1310
2	110	1:50	0.2357
15	110	1:50	0.3074
8	100	1:30	0.2280
8	100	1:30	0.2903
8	100	1:30	0.3543
8	100	1:30	0.3614

MnL_2: manganese laurate; MNK: methyl nonyl ketone (undecan-2-one).

As seen in Figure 4, the main effect and interaction effects involving the variable temperature have a negative effect in this system, which is directly related to the volatilization of the substrate, MNK, in the autoclave reactor during adsorption tests. When the temperature increases, more molecules migrate to the gas phase, reducing the contact with the adsorbing material, which reduces the concentration of MNK in the metal monocarboxylate matrix. Nevertheless, the effects of molar

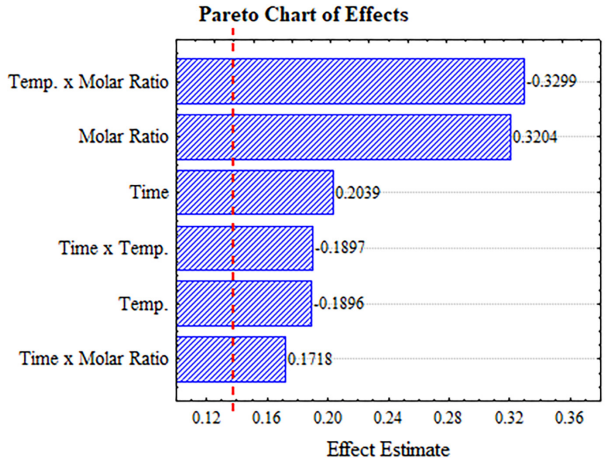

Figure 4. Pareto chart of effects obtained for MNK adsorption in MnL_2.

ratio and contact time positively contributed to the system since they stimulated the interaction of MNK with the MnL_2 matrix. The main effect of molar ratio and its interaction with temperature are highlighted as the most significant factors, indicating that the adsorption mechanism of MNK in the matrix highly depends on these factors.

Figure 5 displays the surface responses for the factor molar ratio *versus* temperature at different contact times. Two main characteristics of the system can help to explain the surface responses: the volatilization of MNK and its affinity to the solid matrix. When the quantities of MNK increase, more species are in contact with the matrix and considering the chemical affinity of these two components caused by the saturated carbonic chains present in both compounds, it is expected that compatible intermolecular forces favor the adsorption.[33] With increasing temperatures, the quantity of MNK present in the liquid-solid interface decreases because this compound goes to the gas phase (as related above), which reduces the contact between the metal monocarboxylate matrix and the substrate.

Figure 5a displays an inconsistency if compared to the other two response surfaces since more adsorption was observed in higher temperatures and lower molar ratios (bottom right corner of the plot). This result is explained by the interaction effect between the variables since the main effect of temperature has a negative effect. In this case, this interaction can be explained as follows; probably, at short times of contact between MNK and matrix and at low molar ratios, higher temperatures can reduce the packing density of the organic chains in the manganese laurate, facilitating the substrate permeation into the matrix.[21] However, this is not a usual response, as observed in subsequent experiments with higher contact times; this is observed only in short contact times (2 days), and after that, desorption processes are favored with the increase in temperature.

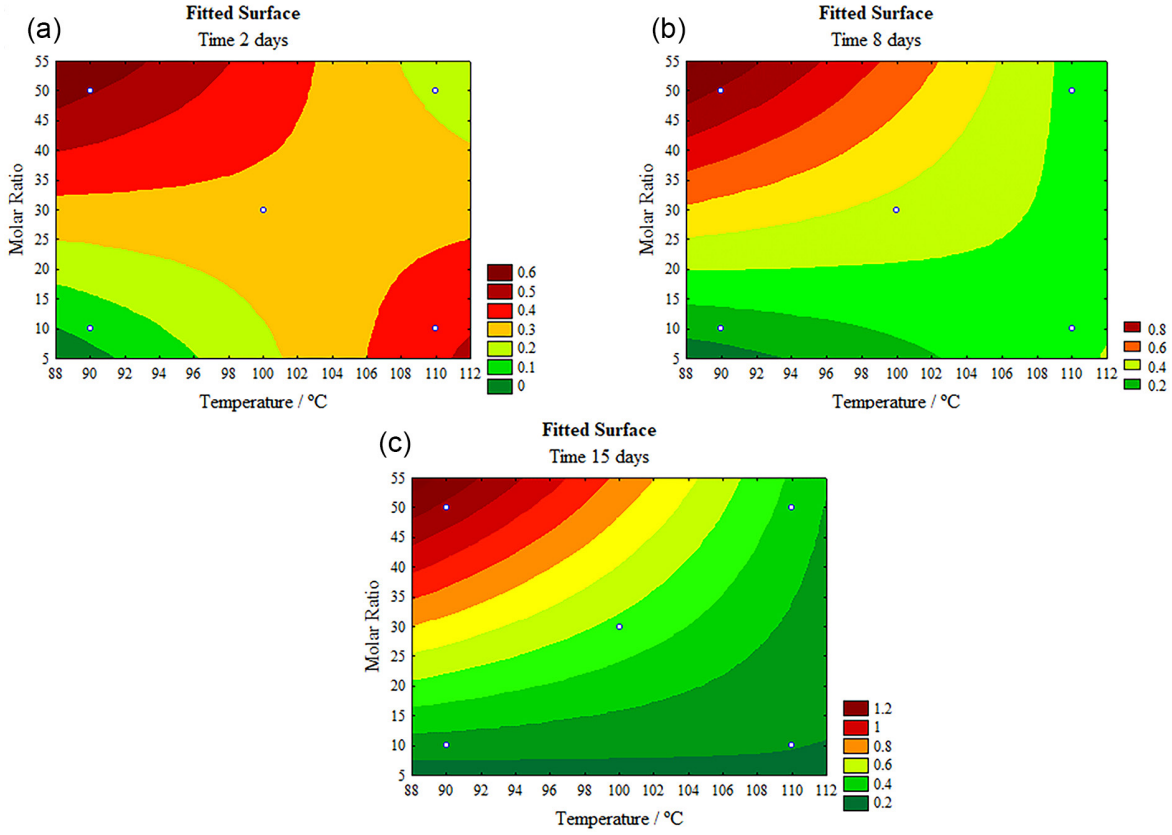

Figure 5. Surface response for molar ratio *versus* temperature at (a) 2, (b) 8 and (c) 15 days obtained for MNK adsorption in MnL_2.

The interaction effects between temperature and time are shown in Figure 6, and the responses indicate that the efficiency of adsorption is more pronounced at lower temperatures and increasing contact times. At low temperatures, fewer MNK molecules are in the gas phase, which favors the contact between matrix and substrate. Moreover, if the contact is made at longer contact times, the interaction between the components is favored, resulting in more adsorption.

Figure 6a depicts an unexpected behavior that evidences the interaction between the variable temperature and time, similarly to the one observed in Figure 5a. This observation implies that at lower molar ratios an increase in temperature can promote adsorption. This can be explained considering that the reduction of the matrix packing density caused by the increase in temperature can promote the substrate-matrix interaction even at lower substrate concentrations. The observed phenomenon indicates that, under these conditions, the volatilization of MNK does not prevail and the reduction in the packing density caused by the temperature can compensate for volatilization processes. Also, at lower molar ratios, the matrix solubility in the substrate is probably less prominent since it can act like a solvent too in the reaction medium.

The interaction effects of molar ratio *versus* time of contact are shown in Figure 7. The responses are higher with longer times of contact, and the adsorption of MNK in the metal monocarboxylate matrix is favored. This is expected regarding the intermolecular forces involved and compatibility between the substrate and the layered manganese monocarboxylate matrix.

In Figure 7c, it is possible to observe that at 110 °C, lower molar ratios can lead to higher adsorption. Similar to the discussed for Figure 6a, this response can be related to two factors: a decrease in the matrix packing density with the increase in temperature and a decrease in the solubilization of the matrix in the substrate, which favors the contact between them.

Conclusions

The main conclusions of this work are related to how the matrix of the layered manganese laurate (MnL_2) adsorbs MNK molecules on its surface. Although an intercalation process between this substrate and the matrix was not observed, the adsorption phenomenon occurred and was investigated in a design of experiments. The adsorption is negatively influenced by an increase in temperature, mainly due to the substrate volatilization that reduces

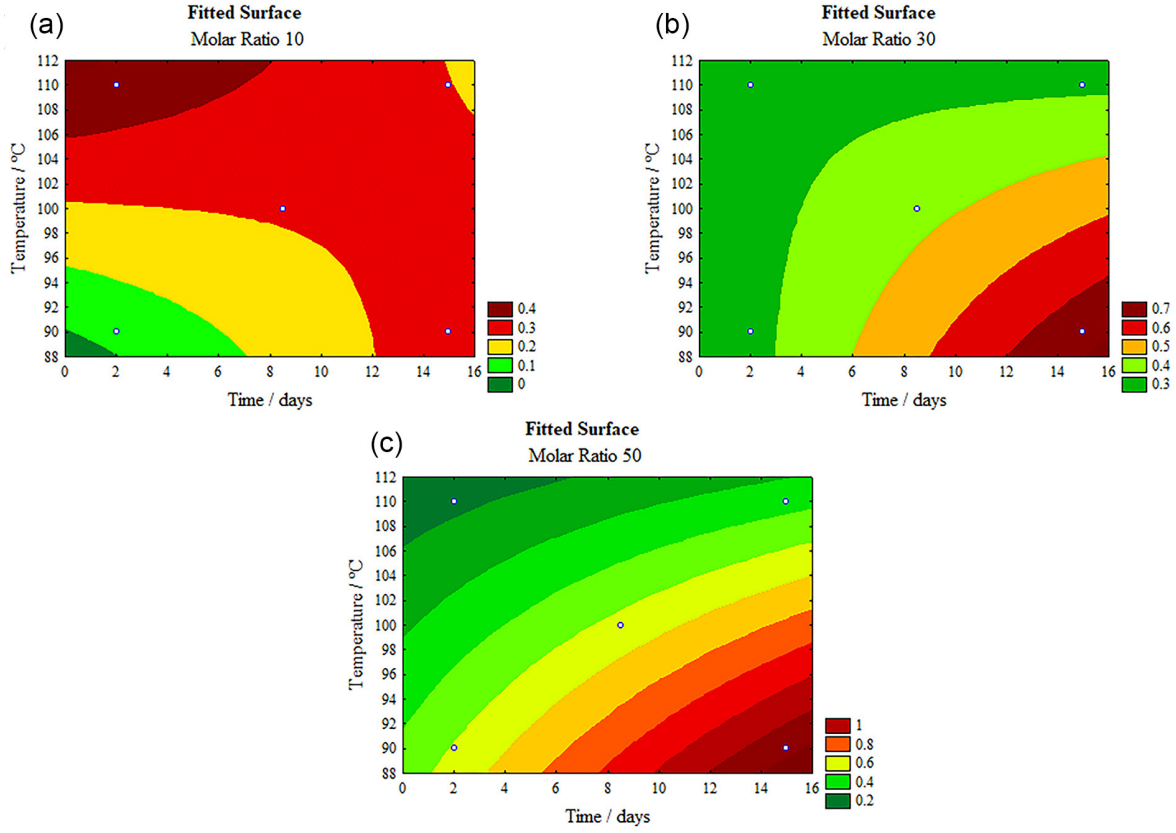

Figure 6. Surface response for temperature *versus* time at molar ratios (MnL_2:MNK) of (a) 1:10, (b) 1:30 and (c) 1:50 obtained for MNK adsorption in MnL_2.

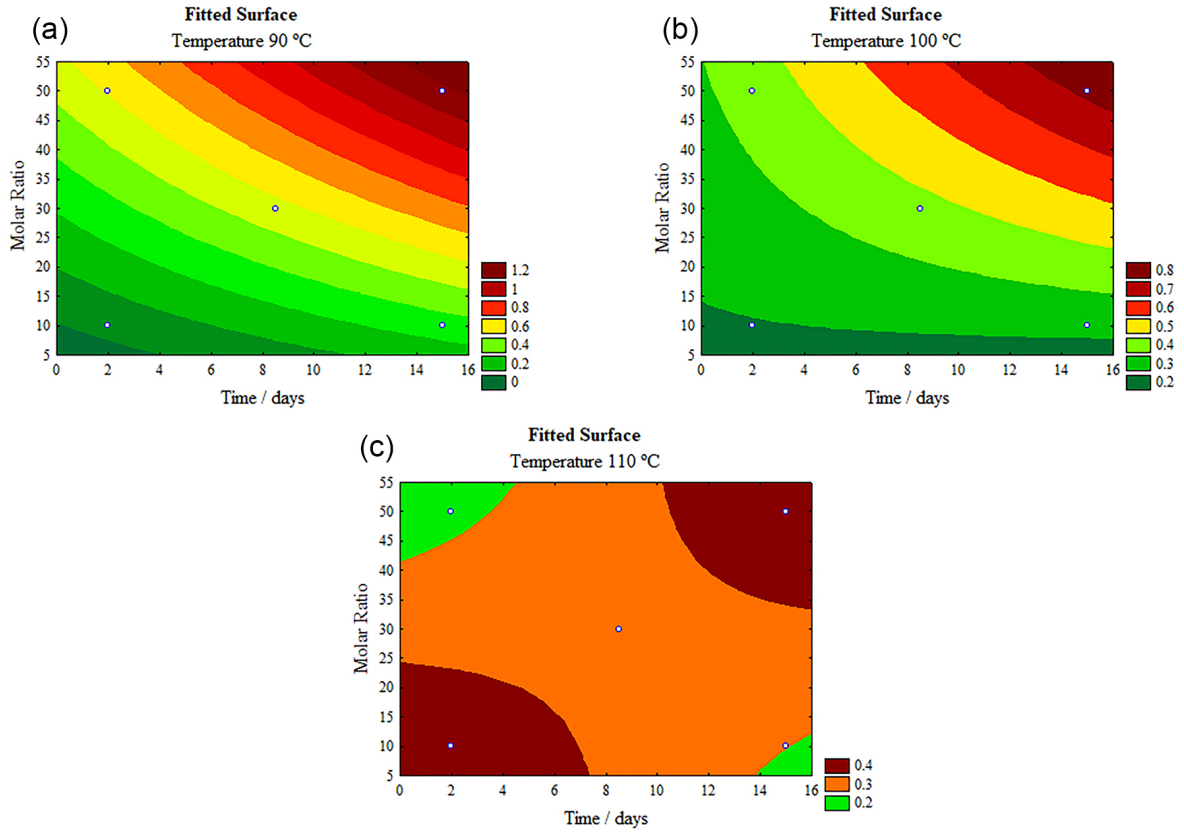

Figure 7. Surface response for molar ratio *versus* contact time at the temperatures of (a) 90, (b) 100 and (c) 110 °C obtained for MNK adsorption in MnL_2.

the solid-liquid interface between the two components. However, with increasing molar ratios and times of contact, adsorption is favored, which suggests that the manganese laurate is a promising material for slow-release tests for pheromone components containing molecules with chemical similarities.

Supplementary Information

Supplementary data are available free of charge at http://jbcs.sbq.org.br as PDF file.

Acknowledgments

The authors would like to thank the Federal University of Itajubá (UNIFEI), the Institute of Physics and Chemistry (IFQ), the Structural Characterization Laboratory from UNIFEI (LCE), the Foundation for Support Research of the State of Minas Gerais (FAPEMIG) and the Chemical Mining Network of Minas Gerais for the research support.

Author Contributions

Anderson N. de Carvalho was responsible for formal analysis, investigation, methodology, data curation, writing original draft; Mirelly A. Vaz Fonseca for investigation, methodology; Diogo M. Vidal for formal analysis, writing original draft; Ana Cristina T. Cursino for methodology, data curation; Daniele S. Firak for investigation, data curation, supervision, writing review and editing; Fabio S. Lisboa for conceptualization, formal analysis, data curation, project administration, resources, supervision, writing original drafts, review and editing.

References

1. Zarbin, P. H. G.; Rodrigues, M. A. C. M.; Lima, E. R.; *Quim. Nova* **2009**, *32*, 722. [Crossref]
2. Instituto Brasileiro de Geografia e Estatística (IBGE); Censo Agropecuário, https://sidra.ibge.gov.br/tabela/9024, accessed in January 2023.
3. de Souza, M. T.; de Souza, M. T.; Rizzato, F. B.; Zawadneak, M. A. C.; Cuquel, F. L.; *Crop Prot.* **2019**, *119*, 180. [Crossref]
4. Cuenca, J. B.; Tirado, N.; Barral, J.; Ali, I.; Levi, M.; Stenius, U.; Berglund, M.; Dreij, K.; *Sci. Total Environ.* **2019**, *695*, 133942. [Crossref]
5. Moliterno, A. A. C.; Martins, C. B. C.; Szczerbowski, D.; Zawadneak, M. A. C.; Zarbin, P. H. G.; *J. Chem. Ecol.* **2017**, *43*, 550. [Crossref]
6. Heuskin, S.; Verheggen, F. J.; Haubruge, E.; Wathelet, J.-P.; Lognay, G.; *Biotechnol., Agron., Soc. Environ.* **2011**, *15*, 459. [Crossref]

7. Tiboni, A.; Coracini, M. D. A.; Lima, E. R.; Zarbin, P. H. G.; Zarbin, A. J. G.; *J. Braz. Chem. Soc.* **2008**, *19*, 1634. [Crossref]
8. Arizaga, G. G. C.; Satyanarayana, K. G.; Wypych, F.; *Solid State Ionics* **2007**, *178*, 1143. [Crossref]
9. Laipan, M.; Xiang, L.; Yu, J.; Martin, B. R.; Zhu, R.; Zhu, J.; He, H.; Clearfield, A.; Sun, L.; *Prog. Mater. Sci.* **2020**, *109*, 100631. [Crossref]
10. Borges, R.; Prevot, V.; Forano, C.; Wypych, F.; *Ind. Eng. Chem. Res.* **2017**, *56*, 708. [Crossref]
11. Borges, R.; Wypych, F.; *J. Braz. Chem. Soc.* **2019**, *30*, 326. [Crossref]
12. Borges, R.; Wypych, F.; Petit, E.; Forano, C.; Prevot, V.; *Nanomaterials* **2019**, *9*, 183. [Crossref]
13. Hermans, J. J.; Keune, K.; van Loon, A.; Corkery, R. W.; Iedema, P. D.; *RSC Adv.* **2016**, *6*, 93363. [Crossref]
14. Lisboa, F. S.; Gardolinski, J. E. F. C.; Cordeiro, C. S.; Wypych, F.; *J. Braz. Chem. Soc.* **2012**, *23*, 46. [Crossref]
15. Otero, V.; Sanches, D.; Montagner, C.; Vilarigues, M.; Carlyle, L.; Lopes, J. A.; Melo, M. J.; *J. Raman Spectrosc.* **2014**, *45*, 1197. [Crossref]
16. Nelson, P. N.; Taylor, R. A.; *Appl. Petrochem. Res.* **2014**, *4*, 253. [Crossref]
17. Barman, S.; Vasudevan, S.; *J. Phys. Chem. B* **2006**, *110*, 22407. [Crossref]
18. Gao, J.; Ye, K.; He, M.; Xiong, W.-W.; Cao, W.; Lee, Z. Y.; Wang, Y.; Wu, T.; Huo, F.; Liu, X.; Zhang, Q.; *J. Solid State Chem.* **2013**, *206*, 27. [Crossref]
19. Akanni, M. S.; Okoh, E. K.; Burrows, H. D.; Ellis, H. A.; *Thermochim. Acta* **1992**, *208*, 1. [Crossref]
20. Gangula, S.; Suen, S.-Y.; Conte, E. D.; *Microchem. J.* **2010**, *95*, 2. [Crossref]
21. Saphanuchart, W.; Saiwan, C.; O'Haver, J. H.; *Colloids Surf., A* **2008**, *317*, 303. [Crossref]
22. Tavares, S. R.; Wypych, F.; Leitão, A. A.; *Mol. Catal.* **2017**, *440*, 43. [Crossref]
23. McBain, J. W.; Sierichs, W. C.; *J. Am. Oil Chem. Soc.* **1948**, *25*, 221. [Crossref]
24. Barman, S.; Vasudevan, S.; *J. Phys. Chem. B* **2006**, *110*, 651. [Crossref]
25. Dou, Q.; Ng, K. M.; *Powder Technol.* **2016**, *301*, 949. [Crossref]
26. Hocking, R. K.; Hambley, T. W.; *Inorg. Chem.* **2003**, *42*, 2833. [Crossref]
27. Sutton, C. C. R.; da Silva, G.; Franks, G. V.; *Chem.-Eur. J.* **2015**, *21*, 6801. [Crossref]
28. Binnemans, K.; Jongen, L.; Görller-Walrand, C.; Olieslager, W. D.; Hinz, D.; Meyer, G.; *Eur. J. Inorg. Chem.* **2000**, 1429. [Crossref]
29. Li, H.; Bu, W.; Qi, W.; Wu, L.; *J. Phys. Chem. B* **2005**, *109*, 21669. [Crossref]
30. Asemani, M.; Rabbani, A. R.; *J. Pet. Sci. Eng.* **2020**, *185*, 106618. [Crossref]
31. Yuan, Y.; Teja, A. S.; *J. Supercrit. Fluids* **2011**, *56*, 208. [Crossref]
32. Nowakowska, M.; White, B.; Guillet, J. E.; *Macromolecules* **1988**, *21*, 3430. [Crossref]
33. Fan, S.; Ruggiero, M. T.; Song, Z.; Qian, Z.; Wallace, V. P.; *Chem. Commun.* **2019**, *25*, 3670. [Crossref]

Submitted: August 1, 2022
Published online: January 10, 2023